

OSMOSE WP3: Factory Acceptance Test of the grid forming demonstrator

Carmen Cardozo,
Guillaume Denis
and Thibault Prevost
RTE R&D
La Defense, France

Email: carmen.cardozo@rte-france.com

Markel Zubiaga,
Alain Sanchez-Ruiz
and Juan Jose Valera
Ingeteam
Bilbao, Spain

Email: markel.zubiaga@ingetteam.com

Yannick Vernay
RTE CNER
Lyon, France
Email: yannick.vernay@rte-france.com

Abstract—In the EU-funded project OSMOSE, RTE and Ingeteam installed a 1 MVA demonstrator to show the technical and economical viability of building a grid-forming function upon a commercially available hybrid energy storage system. In this paper we share the experimental results obtained in a power hardware in the loop test bench during the Factory Acceptance Test. We implemented a filtered droop control with a threshold virtual impedance (TVI) for current limitation. Performance assessment covered synchronisation, reference tracking and disturbance rejection, including low voltage ride-through, phase jumps and grid frequency variations, but also the behaviour under permanent unbalanced and distorted conditions. This demonstrator contributes to increase of the TRL of the grid forming function as the implemented control proved to be effective in providing frequency and voltage smoothing services while operating safely without oversizing and compiling with most of the current technical requirements.

I. INTRODUCTION

One of the objective of the Work Package 3 (WP 3) of the OSMOSE project is to increase the technology readiness level (TRL) of the grid-forming solution by deploying 2 utility-scale demonstrators:

- 1) an existing 720 kVA/560 kWh Lithium-Titanate (LTO) battery installed at the EPFL campus already used for experimental activities [1] and that has been turned into grid-forming, and
- 2) a 1 MVA grid-forming converter backed up by an hybrid energy storage system (HESS) built by Ingeteam and connected to the RTE network in September 2020.

This paper shares experimental results of the latter obtained during the factory acceptance test (FAT) conducted in July 2020 using a power hardware in the loop set-up in the Ingeteam Power laboratory in Zamudio, Spain.

Other objectives of this WP include showing the compatibility of the grid forming function with other services and explore the possibility to pool different storage units that provide specific services through one AD/DC interface.

A. Functional specifications

In this section we summarise the main technical specifications applied to the demonstrator and verified during FAT. They are based on current requirements for the connection of non synchronous energy storage systems (ESS) under discussion in France and the recommendations of the MIGRATE project for the grid forming function in particular [2].

They are consistent with latest recommendations for inverter based resources (IBR) at European level which suggest an alignment with other existing Connection Network Codes (CNC) [3], mainly Requirements for Generators (RfG) and High Voltage Direct Current (HVDC).

- **Active power reference tracking.** CNCs do not enforce any explicit requirement on active power tracking, but we expect dynamics comparable to current grid connected applications associated to ESS or renewable energy sources (RES), which are generally below 500 ms, with limited overshoot and settable ramp.
- **Voltage regulation services.** The system must receive a voltage reference U_{ref} with a settable reactive power droop λ so that $U_{ref} = U + \lambda Q$, where U is the voltage at the connection point and Q the injected reactive power. In France, HVDC CNC requests settling time for primary voltage regulation below 2 seconds.
- **Frequency regulation services.** The system must be able to participate to:
 - 1) Primary frequency regulation with a settable droop K_{FCR} . Response time should be below 30 seconds as enforced in continental Europe (CE), with an activation time below 500 ms for IBR.
 - 2) Enhanced frequency response with settable droop K_{EFR} . Response time should be below 1 seconds as enforced in UK [4]
- **Inertia.** The system must provide instantaneous active power following a grid frequency deviation. The contribution and the dynamic of the recovery of the previous active power set point is settable with two parameters: an electrical inertia H_e and a time constant T_{gf} .
- **Low Voltage Ride Through capability.** The system must maintain a balanced 50 Hz voltage source behaviour during voltage dips¹. The voltage amplitude can be reduced to ensure current limitation. We consider the profile applied in France for a power-generating module type C, which is a 95% voltage dip for 150 ms, and any low voltage above the line between this value and 85% of the nominal voltage after 1.5 seconds.
- **Fast active power recovery.** We take 150 ms as a 90% rise time, and 200 ms settling time to 95% after a reference fault case (95% U dip for 150 ms).

¹In this project we required a synchronous machine-like behaviour. However, the control could be adapted to consider different support strategies.

- **Fault current injection.** No over-sizing is foreseen in this project so the current will remain around its nominal value during faults. As a consequence of the requested voltage source behaviour:
 - 1) There is not any explicit control law that establish an active/reactive current prioritisation during the fault. It will depend on the system impedance.
 - 2) The negative sequence current is naturally prioritised, although different strategies were studied.
- **Harmonics.** The converter must withstand the presence of grid voltage background harmonic, without injecting adverse harmonic. More sophisticated active filtering strategies could be proposed to better fit the specific needs of a given location, but for the moment we have left this topic out of the scope of the project.
- **Degraded modes.** The grid forming function must exhibit the same behaviour independently of the DC side energy source, whether the HESS is available, or only the supercapacitances or the battery are connected.
- **Multiservices.** An active power reference signal, P_{set} , is computed by an external controller and can be sent at least every second through modbus protocol. However, a settable energy budget (SoC_{min} and SoC_{max}) is reserved for grid forming. When one of these thresholds is reached, all other services that push the SoC beyond this limit are blocked.
- **State of Charge.** The supercapacitors SoC is constantly regulated from the battery with a settable dynamic (≈ 1 minute). An hysteresis control automatically restores the SoC of the battery if extreme values are reached and if the network is at normal state. A continuous control is also available to regulate the SoC of the battery to a predefined value with a slow dynamic (≥ 1 hour).

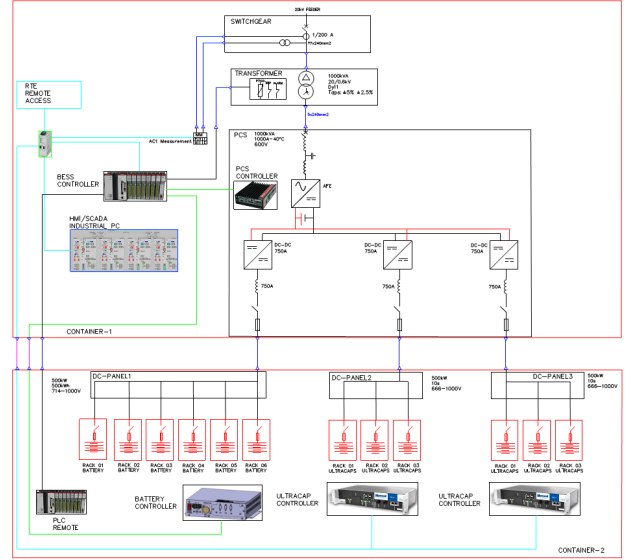


Fig. 1. Demonstrator diagram

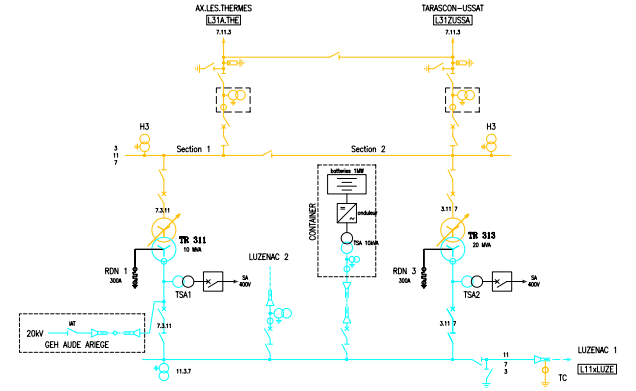


Fig. 2. Demonstrator connection in Castelet substation

B. Demonstrator description

Ingeteam provided a 1 MVA rated power fully containerised solution as showed in fig. 1, which include:

- Four lithium-ion battery racks (0.5 MVA 60 min),
- two times three ultracapacitor racks (1MW-10s),
- 3 x 500 kW DC/DC converters,
- 1 MVA Low Voltage (600V) AC/DC converter,
- 1 MVA 0.6/20 kV transformer, and
- a medium voltage switchgear cubicle.

The HESS has been installed at the 20 kV bus bar of the Castelet substation in the south of France, which includes:

- a 63 kV line to Aix Les Thermes substation,
- a 63 kV line to Tarascon-Ussat substation,
- a 10 MVA 63/20 kV transformer dedicated to a power hydro generation unit,
- a 20 MVA 63/20 kV transformer for the power supply of an industrial consumer with underground cable, where the demonstrator will be connected (see fig. 2).

C. Grid forming control settings

In this project, the filtered droop grid-forming control proposed in the MIGRATE [5] is implemented. It does not consider a phase-locked loop (PLL). The current limitation is based on a Threshold Virtual Impedance (TVI) and the droop is reduced during its activation [6].

Previous works showed the stable association of the grid forming function with different DC side power sharing and energy management strategies [7] and a preliminary performance assessment on EMTP [8] anticipates proper behaviour with the connection grid. This section recalls main features and settings selected for the final control:

- The outer active power control consists in a filter droop with two settable parameters: ω_c and m_p . The equivalent electrical inertia is defined as $H_e = \frac{1}{2\omega_c m_p}$ and P is the positive sequence injected power.

$$\dot{\omega} = \omega_c (\omega_{set} + m_{p,var} (P_{set} - P) - \omega) \quad (1)$$

$$m_{p,var} = m_p \left(\sqrt{(1 - \Delta e_{gd,TVI})^2 + \Delta e_{gd,TVI}^2} \right)$$

- The outer voltage control consists in a reactive power droop with settable parameter n_q , where E_{ref} is the converter output voltage reference and Q is the absorbed positive sequence reactive power.

$$E_{ref} = E_{set} + n_q (Q - Q_{set}) \quad (2)$$

- A primary frequency controller with a settable dynamic T_{FR} and droop (K) is implemented on top of the grid forming control, such that:

$$P_{ref} = P_{set} - K (f - f_0) \quad (3)$$

- An upper loop has been added to slowly adapt the frequency set point to the droop output in order to ensure active power reference tracking in steady state and no interference with any multi service optimisation strategy. The dynamic is set with the T_{GF} time constant.

$$\dot{\omega}_{set} = \frac{1}{T_{GF}}(\omega - \omega_{set}) \quad (4)$$

- TVI current limitation strategy reduces the converter voltage reference proportionally to the current when the threshold (I^{th}) set to 1.2 p.u., is reached as indicated in (5). There is not any switch to current control.

$$\Delta e_{gd,TVI} = \begin{cases} Kp_{TVI} \left(\sqrt{i_{sd}^2 + i_{sq}^2} - I^{th} \right) (i_{sd} - D_{XR}i_{sq}) & \text{if } I_s \geq I^{th} \\ 0 & \text{otherwise} \end{cases}$$

$$\Delta e_{gq,TVI} = \begin{cases} Kp_{TVI} \left(\sqrt{i_{sd}^2 + i_{sq}^2} - I^{th} \right) (i_{sq} + D_{XR}i_{sd}) & \text{if } I_s \geq I^{th} \\ 0 & \text{otherwise} \end{cases} \quad (5)$$

D. Operation of the demonstrator

Standard grid following control is available, but it can only be activated by HMI command at the starting of the installation. The system is designed to always operate in grid forming independently of the network conditions.

The system can be energised from both the DC side or the AC side. Both options were tested, but only energisation from the AC will be authorised in operation. Analogously, the islanding function has been tested but will not be used in operation. The converter have been programmed to stop when the system operator open the 20 kV breaker inside the switchgear cubicle.

Set points and ramps can be manually set from the HMI or remotely from an external controller through modbus protocol in order to include multi-service optimisation [9].

Different DC side power sharing settings are available: a) slow, b) medium and c) fast which lead to an increase in the battery participation to the transients. In addition, it is possible to operate the system with only one storage technology. In case of operating with only supercapacitor, all energy intensive services (P_{set}) including frequency regulation are blocked. A continuous state of charge control restore the reserve level within about 1 minute.

Transient fault recorders (TFR) have been installed at the 20 kV feeder and at the medium voltage switchgear cubicle to isolate the contribution of the demonstrator. In addition, the converter control and protections system (PCS) includes a TFR at converter side.

II. FAT DESCRIPTION

The scope of the demonstrator FAT for the grid forming function includes the converter with its output filter, as well as the DC side converters and filters.

A. Test bench description

The AC/DC converter is connected to a 0.7 MW rated power grid emulator that represents the network through a controlled voltage source behind a virtual reactance. Each DC/DC converter is connected to one rack of battery / supercapacitors.

- A sequence separation is performed but the use of decomposed signal is limited as delays associated to this treatment led to performance loss, especially for transient events. Hence, the implementation of a full negative sequence control loop was excluded at the final stage of control design. As a consequence, the share between positive and negative sequence current is not settable. Moreover, special attention was given to the computation of the current peak (I_s) for TVI activation criteria to prevent intermittent switching when injecting harmonic currents.

Limited by the current capability of the grid emulator (650 A), the tests are performed at reduced power: the base power and voltage are set to 138 kVA and is 220 V respectively. The virtual grid filter adds a 11.6 % connection impedance (Lf=130uH, Cf=200uF and Rf=0.1 ohm). Hence, the results are representative of the demonstrator connected to a system of $SCR \approx 20$ (the low voltage transformer reactance is 6.2%).

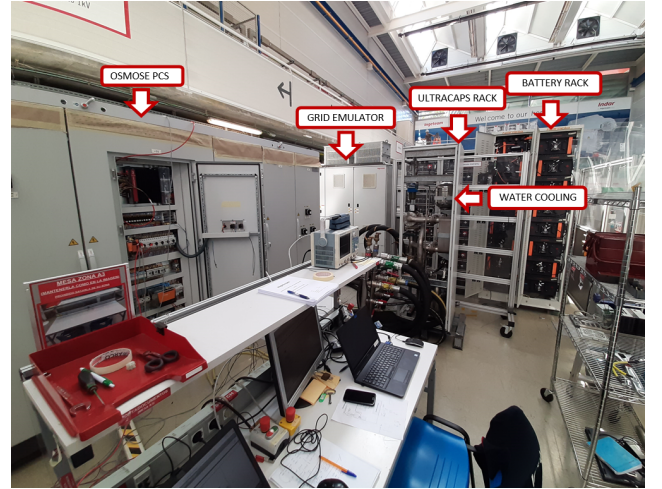


Fig. 3. Experimental environment

B. Test description

The tests are mainly **perform** at power references set to zero to focus on the transient response. An offset in the active power is observed in some tests due to the activation of the battery SoC control. Default parameters are $\omega_c = 25$ rad/s and $m_p = 0.01$ p.u. for $H_e = 2s$. H_e equal to 5 s can be obtained for $\omega_c = 20$ rad/s and $m_p = 0.005$ p.u. The steady state power is defined through P_{set} .

C. Recorded signals

FAT records include two phase-to-phase instantaneous converter voltages and the three phase currents. Here we report active and reactive, positive and negative sequence components calculated according to [10] and [11]. In some tests we include measurements of DC side quantities.

III. EXPERIMENTAL RESULTS

A. Synchronisation & islanding

For this test, the converter was energised from the DC side. When the breaker is open, the synchronisation algorithm imposes the voltage reference to be equal to the grid voltage (here 1.05 pu). Immediately after the breaker closing, the user defined reference is imposed (here 1 pu) generating a reactive power exchange. As expected, a well damped active power transient lead to proper synchronisation in less than 300 ms. Figure 5 illustrates the grid forming converter voltage source behaviour after breaker opening.

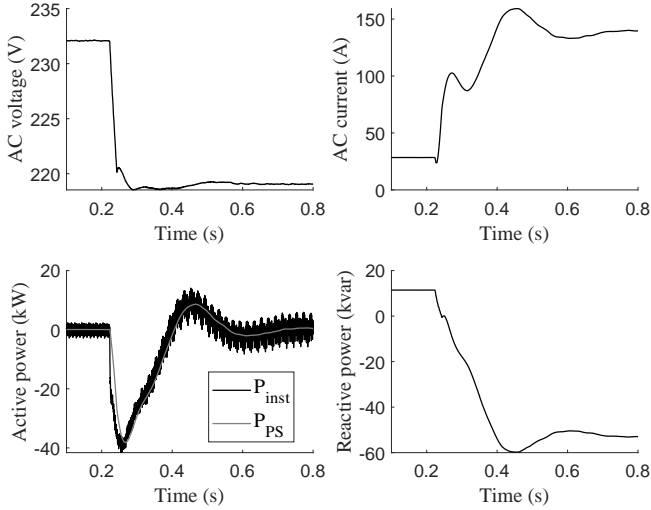


Fig. 4. Connection to the grid for $V_g=1.05$ p.u. $E_{set}=1$ p.u.

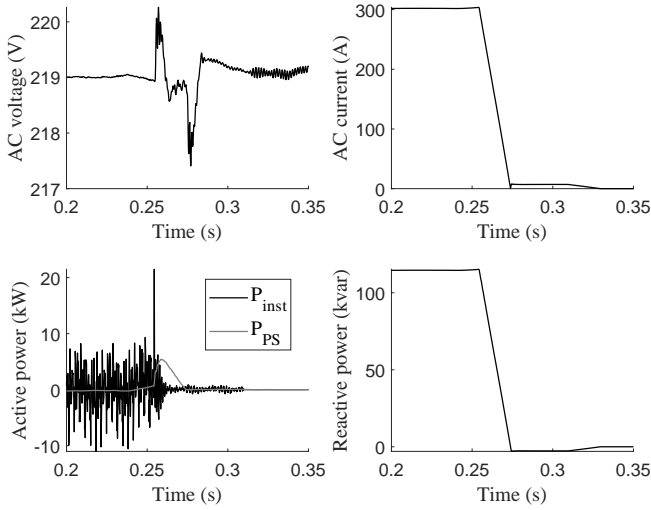


Fig. 5. Islanding while injecting maximal reactive power

B. Reference tracking

1) *Voltage reference step:* The voltage reference is tracked within 100 ms with good dynamics, independently of the reactive power droop (n_q). Figure 6 shows that the active power return to the set point after a 200 ms transient. In operation, ramp limits are applied to the set points as shown in fig. 7 for a modification of the reactive power set point which lead to smoother behaviours.

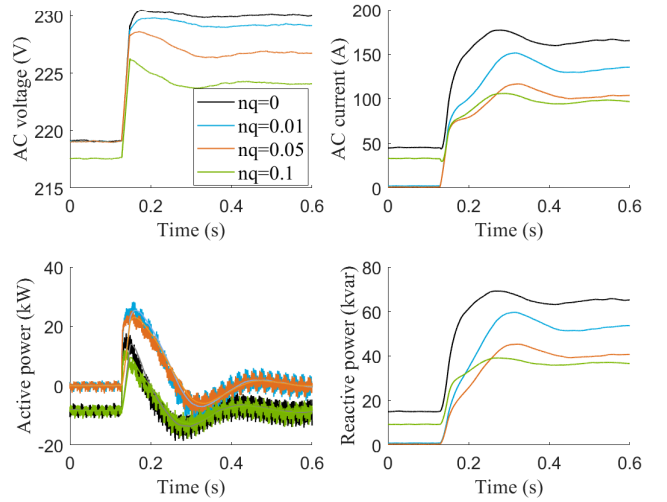


Fig. 6. 5% Step on voltage set point ($H=2$ s)

2) Reactive power ramp:

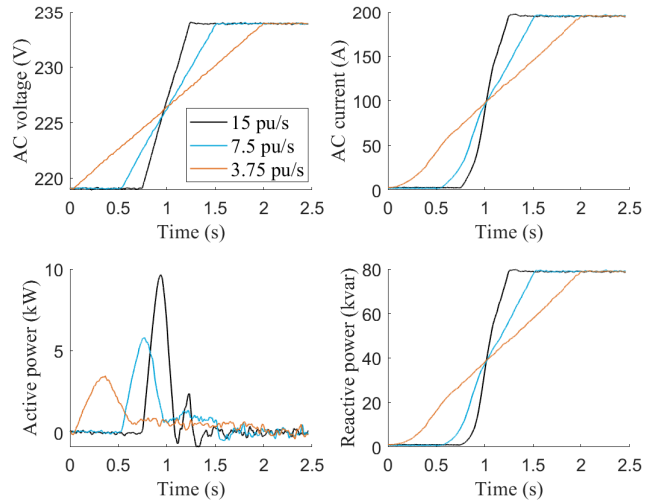


Fig. 7. 80 kvar with different ramps for $n_q=0.01$ ($H=2$ s)

3) *Active power ramp:* The well known oscillatory nature of the filtered droop appears for high active power ramps as shown in fig. 8.

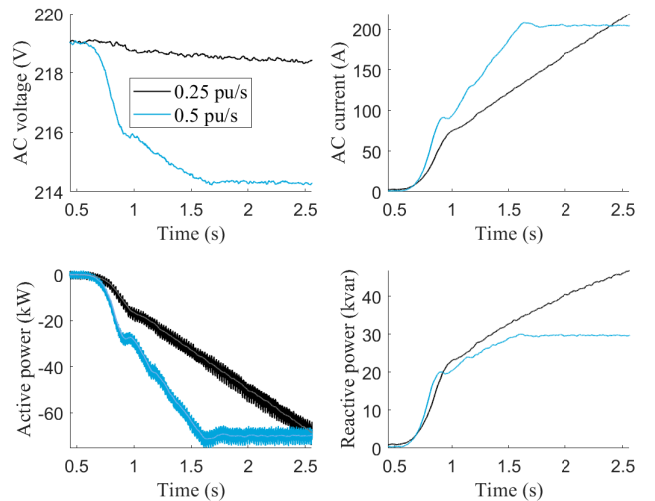


Fig. 8. -70 kW active power ramp ($H=2$ s, with different n_q)

C. Disturbances

1) *Phase jump*: we assess three different configurations: a) 3 DC-DC converters connected, b) the battery DC-DC converter disconnected (Only UC) and c) both DC/DC supercapacitors converters disconnected (Only Bat). The control parameters of the DC/DC controller automatically switch to a degraded mode settings. As expected, the three configurations exhibit the same behaviour from the AC side. Due to the high inertia, the response to a 5° phase jump shown in fig. 9 yielded almost 70% of nominal active power.

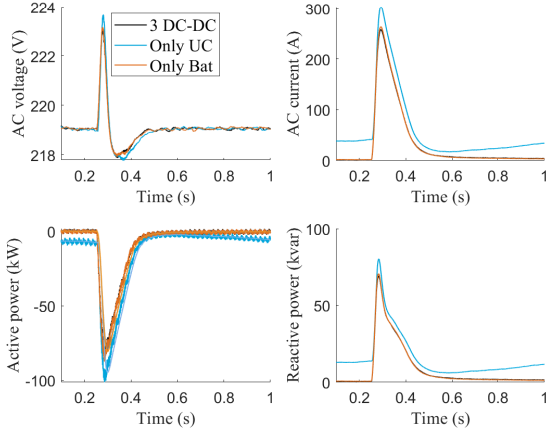


Fig. 9. 5° phase jump ($H = 5$ s)

2) *Symmetric voltage dips*: fig. 10 shows three different tests: a) 100% for 250, b) 75% for 500 ms and c) 50% 700 ms. The residual voltage is due to the filter impedance. The low system resistance combined with a voltage source behaviour results in a high share of reactive current without any explicit control law defining a prioritisation strategy. The TVI successfully limited the current to acceptable values in all cases. The recovery time after fault clearance depends on control parameters (inertia) and fault depth and duration. The adaptive droop proved to be effective in increasing critical clearing time (CCT) and helped to keep active power recovery within 200 ms.

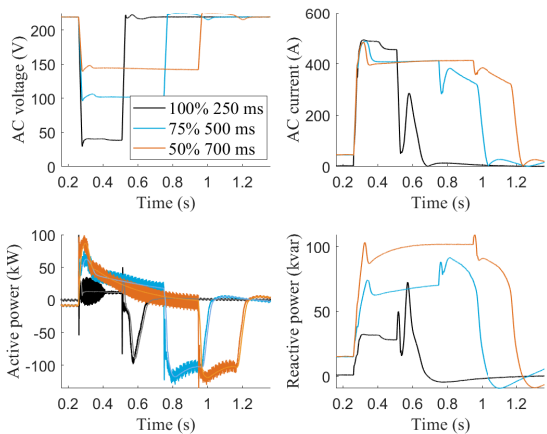


Fig. 10. Symmetric fault ride through capability ($H = 2$ s)

3) *Asymmetric voltage dip*: we present here the response to a type C voltage dip which represents a phase-to-phase fault or a single phase fault after a transformer connected in star-delta. The voltage unbalance is slightly reduced at the converter terminals which lead to high unbalance in the current. The TVI is again effective in protecting the device while allowing negative sequence reactive current to flow.

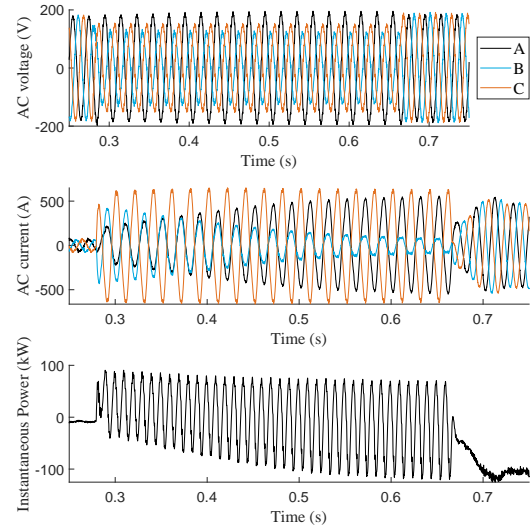


Fig. 11. 50% Type C voltage dip for 400 ms

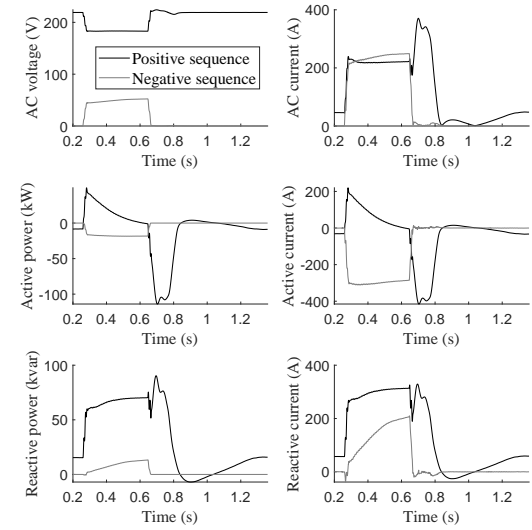


Fig. 12. 50% Type C voltage dip for 400 ms

D. Robustness to harmonics

The virtual grid was set to produce a high (beyond expected on grid) voltage distortion: 10% of the 5th harmonic.

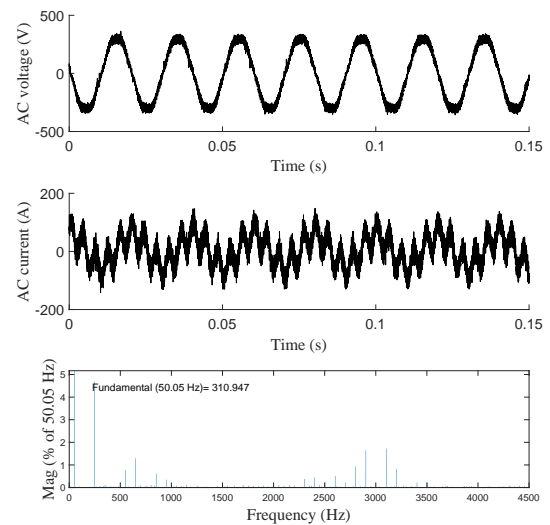


Fig. 13. 10% of 5th harmonic distortion

The grid forming converter absorbs large harmonic current and reduce the voltage distortion from 10% in the grid to 4% at its terminals associated to the filter's impedance.

E. Power sharing between storage devices

DC side converters parameters can be chosen to define different power sharing strategies. The default mode is the "slow" one which ensures that the power peak is provided by the supercapacitors while the battery ramps slowly after a power step for instance. As the battery control is accelerated, the DC voltage can be regulated to a tighter band. For any of the three settings, the DC voltage is regulated with 1% which illustrates the decoupling of the DC side dynamics from the network provided by the active parallel hybrid topology. As a consequence, the AC/DC converter gives the same response.

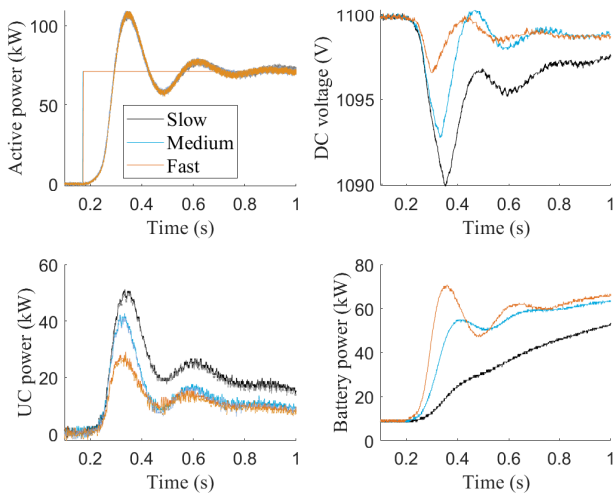


Fig. 14. 70 kW active power step ($H = 2$ s)

F. Frequency regulation services

In this test, the frequency controller is disabled so only the inertial response is observed. Following a 200 mHz step applied to the grid emulator frequency, the converter instantaneously provides active power. The fast transient is absorbed by the supercapacitors with low impact on the DC voltage, and their contribution is reduced as the battery takes over. Then, the battery will also reduce the active power with a settable dynamic proving that grid forming function is compatible and can be decoupled from other services.

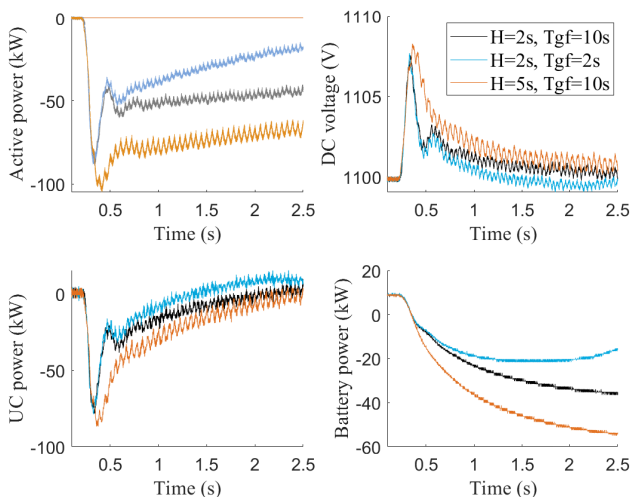


Fig. 15. Grid frequency deviation: battery power stabilises at 0 after 10 s

For $H = 5$ s the disturbance was limited to 150 mHz to avoid TVI activation.

IV. CONCLUSIONS

Specific Factory Acceptance Tests to validate the proper behaviour of the grid forming control of the RTE - Ingeteam demonstrator were successfully performed in July 2020 using a power hardware in the loop platform available at the Ingeteam Power Laboratory in Zamudio, Spain. The system has been delivered during the summer and connected to the RTE network at the end of September 2020.

Low voltage ride through capability and fast fault current injection proven to be compliant with MIGRATE recommendation and most requirements proposed in the UK grid code draft for grid forming plants [12], i.e. high reactive current is injected immediately (starts to rise in less than 5 ms) during voltage dips as a consequence of the voltage source behaviour, even when current limitation is reached (with TVI). However, some active current might still flow depending on the system impedance. Moreover, the phase, voltage magnitude and frequency are not fixed to their pre-fault value during low voltage events. Indeed the voltage magnitude is reduced by the TVI to achieve current limitation and the phase does tend to drift but quite slowly due to the reduction of the active power droop.

Inertia active power, defined in [12] as the inherent capability to respond naturally, within less than 5 ms, to System Phase and Frequency changes without any supplementary control, was also verified. The contribution can be adapted through settable control parameters. However, the well known oscillatory behaviour of this type of grid forming controls was observed. The natural mode frequency and damping varies with the control parameters. A compensation term (P_s) can be computed by the external controller to improve damping [13] such that $P_{set} = P_{sp} + P_s$.

The installation also proven to be robust to unbalance (5% permanent unbalance tested) and distorted network conditions (10% of 5th harmonic and 7% of 7th harmonic). Future work will address remaining challenges on robust negative sequence, damping and active filtering control design in grid forming mode. For this purpose a frequency dependent impedance model of the demonstrator will be built. In addition, results on the characterisation of the grid forming function from external measurements are expected from the definition of key performance indicators (KPI) that quantify the services provided by grid forming converters.

Next year, we will focus on the operation of the demonstrator connected to the grid as well as EMT studies using the validated models to further investigate extreme conditions. Moreover, the compliance with current grid code drafts for the grid forming capability of other types of controls such as the dispatchable Virtual Oscillator (dVoC) and current limitation strategies will be assessed. Main expected outcomes of the demonstrator operation include: a) recommendation for non-intrusive grid forming specification as well as criteria for certification and performance control, b) model requirements for stability analysis and c) metering needs to enable continuous monitoring.

ACKNOWLEDGMENT

This work is part of the OSMOSE project. The project has received funding from the European Union's Horizon 2020 research and innovation program under grant agreement No 773406. This article reflects only the authors views and the European Commission is not responsible for any use that may be made of the information it contains.

REFERENCES

- [1] Namor, Emil, *Advanced models and algorithms to provide multiple grid services with battery storage systems*, 2018, available: <http://infoscience.epfl.ch/record/256959>
- [2] *Deliverable 3.6: Requirement guidelines for operating a grid with 100% power electronic devices..* [Online]. Available: <https://www.h2020-migrate.eu/downloads.html>
- [3] ENTSO-E Storage Expert Group *PHASE I FINAL REPORT*. [Online]. Available: https://www.entsoe.eu/network_codes/cnc/expert-groups
- [4] Enhanced Frequency Response National Grid ESO <https://www.nationalgrideso.com/balancing-services/frequency-response-services/frequency-auction-trial>
- [5] *Deliverable 3.2 Local control and simulation tools for large transmission systems.* [Online]. Available: <https://www.h2020-migrate.eu/downloads.html>
- [6] T. Qoria, F. Gruson, F. Colas, G. Denis, T. Prevost and X. Guillaud, *Critical Clearing Time Determination and Enhancement of Grid-Forming Converters Embedding Virtual Impedance as Current Limitation Algorithm*, in IEEE Journal of Emerging and Selected Topics in Power Electronics, vol. 8, no. 2, pp. 1050-1061, June 2020.
- [7] C. Cardozo, G. Denis, T. Prevost, M. Zubiaga, J. J. Valera, Y. Vernay, *Upgrade of a grid-connected storage solution with grid-forming function*, in 9th Solar & storage integration workshop, 15-16 October 2019, Dublin.
- [8] C. Cardozo, Y. Vernay, G. Denis, T. Prevost, M. Zubiaga, J. J. Valera. *OSMOSE: Grid-Forming performance assessment within multiservice storage system connected to the transmission grid*, in CIGRE session 48, 25th August- 3rd September 2020, Paris.
- [9] Emil Namor, Fabrizio Sossan, Rachid Cherkaoui, Mario Paolone, *Deliverable 3.1 Multi-service control algorithm for converters*, December 2018.
- [10] *IEEE Guide for Test Procedures for Synchronous Machines Part I—Acceptance and Performance Testing Part II—Test Procedures and Parameter Determination for Dynamic Analysis - Redline*, in IEEE Std 115-2009 (Revision of IEEE Std 115-1995) - Redline , vol., no., pp.1-219, 7 May 2010, doi: 10.1109/IEEESTD.2010.5953453.
- [11] *FGW: Technical Guidelines for Power Generating Units. Part 4 Demands on Modeling and Validating Simulation Models of the Electrical Characteristics of Power generation Units and Systems*; Revision 4, September 15th, 2009
- [12] National Grid, *Draft Grid Code – Grid Forming Converter Specification*. [Online]. Available: <https://www.nationalgrideso.com/document/159296/download>
- [13] S. Cherevatskiy, s. Sproul, s. Zabihi, r. Korte, h. Klingenberg, b. Buchholz, a. Oudalov, *Grid Forming Energy Storage System addresses challenges of grids with high penetration of renewables (A case study)*, in CIGRE session 48, 25th August- 3rd September 2020, Paris.